

Parallelized Real-time Physics Codes for Plasma Control on DIII-D

A. Rothstein,^{1, a)} K. Erickson,² R. Conlin,^{1,3} A. Bortolon,² and E. Kolemen^{1,2}

¹⁾*Princeton University, Princeton, NJ, USA*

²⁾*Princeton Plasma Physics Laboratory, Princeton, NJ, USA*

³⁾*University of Maryland, College Park, MD, USA*

A real-time safe multi-threading library was developed on the DIII-D plasma control system to optimize the real-time TORBEAM and real-time STRIDE physics codes. These physics codes are crucial for future fusion power plant operation as they provide information about electron cyclotron wave propagation and heating as well as inform about ideal plasma stability limits. The real-time TORBEAM code executed consistently in under 20 ms while the real-time STRIDE code computes in 100 ms. The multi-threading library developed in this work can be applied to other real-time physics-based codes that will be crucial for the next generation of fusion devices.

Keywords: plasma control, MHD, real-time stability, DIII-D, tokamak, parallelization

I. INTRODUCTION

Tokamaks are currently the most promising path to fusion energy¹, with future reactors such as ITER² and SPARC³ promising net positive energy production. Due to the dynamic nature of a tokamak plasma shot, real-time plasma control systems (PCS) are necessary to maintain confinement and have been the subject of study across many tokamak devices^{3–13}.

With the extreme robustness needed for a fusion pilot plant PCS, significant research has been done on developing real-time physics-based codes useful for plasma control. These include more standard equilibrium reconstruction codes like real-time EFIT¹⁴ and LIUQE¹⁵ to more advanced real-time profile prediction codes in RAPTOR^{16,17} and real-time neutron rate calculation codes¹⁸. Additional work has been done to adapt ray tracing codes such as TORBEAM¹⁹ for electron cyclotron heating (ECH) as well as the magnetohydrodynamic (MHD) stability code STRIDE^{20–23} that can give important information about ideal stability limits. However, while the real-time implementations of these physics codes demonstrate significant latency and throughput performance improvements relative to their offline counterparts, they need well-designed PCS environments to achieve the necessary execution times to be useful for real-time control.

Single core performance bottlenecks present a recurring need in real-time physics codes is for a robust multi-threading library to enable parallelization across CPU cores. In the case of real-time TORBEAM (rt-TORBEAM), the ray trace calculations are independent across gyrotrons, yielding conceptually simple parallelization. While existing multi-threading libraries exist such as the widely used OpenMP²⁴, as discussed later in section II A, these do not target systems requiring deterministic latency, such as would be required for any commercial fusion reactor, and are thus not desirable. This motivates the work done here in developing and implementing a real-time-safe multi-threading library on the DIII-D PCS to run both the TORBEAM and STRIDE codes in real-time.

The rest of the paper is organized as follows: in section II we discuss the constraints of the DIII-D PCS environment and

the implementation details of the real-time multi-threading library. In section III we discuss the implementation of the rt-TORBEAM code on DIII-D utilizing the multi-threading library. In section IV we explain the STRIDE real-time problem formulation and implementation as well as show experimental results before concluding in section V.

II. REAL-TIME MULTI-THREADING LIBRARY

In this section, we first discuss the environment of the DIII-D PCS, then move towards regulations that must exist on a resilient, fusion power plant quality PCS, and finally describe the design of the real-time compatible multi-threading library.

A. PCS Environment

The DIII-D PCS functions with a fixed number of processes that each run on separate CPU cores. In each process, a number of algorithms execute serially within an allotted cycle time. If they cannot complete before this time elapses, undefined behavior can occur and can lead to cascading errors for algorithms across the PCS. Thus, it is critical that individual algorithms have well-defined behavior and deterministic runtime.

Additionally, for production-grade software that will be run on a fusion reactor, the PCS code must be robust to any possible error in a way that there will be no undefined behavior that could crash the overall PCS and lead to a critical failure. For a fusion reactor on the grid, this would mean an unexpected loss in power production or, in a worst case scenario, a full PCS failure could lead to an uncontrolled disruption of the plasma and damage hardware components of the reactor. To avoid this, the PCS code must be clear about how it will execute in the event of any and all edge cases

The OpenMP library²⁴ is an industry standard multi-threading library with roots in the world of high performance computing. While it is excellent for most applications, a robust PCS system is not a safe place to apply this package. Many details of thread creation and work assignment are implementation defined and deferred to the respective compilers, and the OpenMP specification does not give hard real-

^{a)}Electronic mail: arothstein@princeton.edu

time guarantees required for microsecond scale plasma control. There are no known implementations that provide these details either as implementation defined scope. There are various complicated mechanisms that can mitigate some timing issues and reduce latency concerns (thread pinning, lock elision, etc.), but these are all best effort, subject to change across compiler versions, and uniquely configured between compiler implementations.

The logical next possibility to consider would be utilizing GPUs connected to the main PCS CPUs for computationally intensive physics codes. While this is an enticing option, GPUs require significantly higher start-up costs than CPU multi-threading and only make sense when there are hundreds or thousands of parallel computations to be done. As described later in Figure 3 and Figure 5, these physics codes need further development work to benefit from GPU hardware. While the physics codes described in this text would not benefit from GPU processing, a prime example for utilizing GPUs in the PCS would be machine learning models²⁵⁻³¹ that require large matrix operations and can best leverage GPU hardware.

For the code described in section III, the calculations were completed on a system with dual 12-core Intel Xeon Gold 6136 CPUs running at 3.0 GHz. For the code described in section IV, the calculations were run on a system with quad 18-core Intel Xeon Gold 6154 CPUs also running at 3.0 GHz. Both of these systems isolated the cores in use for real-time from other processes. The former system used a stock CentOS 7 environment with limitations on isolation possibilities, while the latter system used a commercial real-time OS from Concurrent-RT called RedHawk. This OS provides complete core isolation, including from the kernel timer interrupt. This reduces latency jitter to the minimum allowed by the hardware.

B. Real-time safe multi-threading library details

The multi-threading library described here was initially developed for the Digital Coil Protection System on NSTX-U using a custom C++11 environment and known as the Bidirectional Atomic Synchronization System³². For the DIII-D PCS, that system was adapted to C11 and redesigned for more flexible operation while still maintaining the original abstraction goals. Notably, the various components of the threading system are unaware of the infrastructure of the calling context. While the C++ implementation used object oriented based callable function objects with type bound arguments, the C implementation resorts to pthread-style function pointers with fixed opaque pointers to contain any desired payloads.

The library works by having a single Manager Thread (the **Manager**) which assigns work units to individual Worker Threads (the **Workers**). This is visualized in Figure 1 with two **Workers**. Note the only limit to the **Workers** count is the available threads from the hardware being used to run the algorithm. In our utilization of this library in the DIII-D PCS, the **Manager** is the same as the main thread for the PCS-controlled CPU. This design decision was made to sim-

plify coordination of background work with the data flow of the PCS algorithm without introducing additional complexities such as futures and promises. The tradeoff for that simplicity is that the PCS CPU blocks waiting for the workers to complete their tasks.

The UML diagram in Figure 1 is split into two stages: the pre-shot, non-real-time initialization stage above the blue horizontal block, followed by the during-shot real-time calculation stage below the blue horizontal block. The during-shot stage repeats until the plasma shot is complete. Forward progression of the algorithm is represented by the black arrows pointing downwards and the repetition of CPU cycles throughout the shot are given by the dark green arrows on the far left and far right that return to the blue horizontal block. The following two subsections describe the algorithm represented in Figure 1.

All communication in this design uses low level atomic variables with acquire-release memory model semantics as specified by the C11 standard. These directly mirror the original design's use of the C++11 memory model for the same purpose. The important guarantee from these atomic operations based on the chosen memory model is that when a particular atomic operation becomes visible in another thread, all previous non-atomic operations are also visible. This model does not guarantee ordering of those non-atomic operations, but ordering for this design is not needed. Critically, this approach avoids higher level abstractions that would otherwise involve the kernel, such as semaphores. While those are conceptually simpler and easier to implement, they unfortunately introduce unacceptable nondeterministic behavior from the kernel.

Of particular importance for this mechanism to work is the bidirectional component of the original implementation. Both the **Manager** and the **Workers** independently notify each other of their status through these atomics, allowing synchronization points at the beginning and end of the critical section. This is analogous, and in fact was modeled after, the Ada language "rendezvous" core feature. Without a rendezvous in both directions, the synchronization would break. This means that threads do spend time spinning idly waiting for other threads to catch up. Balancing workloads to maximize CPU utilization is the job of the developer. Such is the nature of real-time systems, where maximal throughput is secondary while determinism and latency are primary.

1. Pre-Shot Initialization

During the plasma shot set-up, the **Manager** initializes the **Workers** and each of the **Workers** waits for the plasma shot to begin. At this stage, the **Manager** enters the state of completed work where each of the **Workers** has no work (equivalent to having completed all previous work) and is ready to receive new jobs. This is the same state that will be achieved at the end of each CPU cycle during the shot. This begins by setting the variables **Ready** and **Complete** to the total number of **Workers** plus one. Finally, when the shot is about to begin, the **Manager** communicates to each worker that the shot is ready to begin, represented by the green arrow that travels

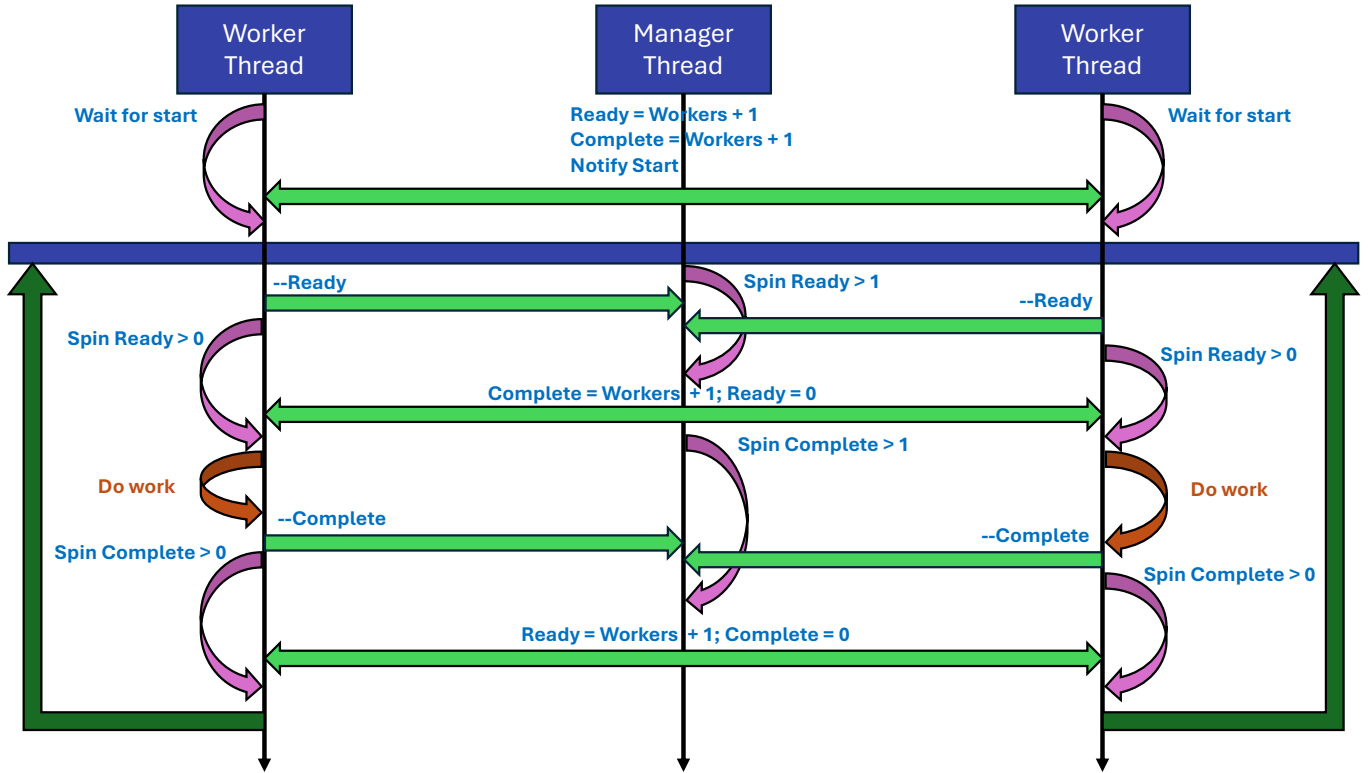


FIG. 1. UML diagram of the multi-threading algorithm. The Manager and Workers each follow the vertical black lines downward to progress through the shot. The horizontal bright green arrows represent communications between the Manager and Workers. An arched pink arrows denotes a thread waiting until some condition X is made *false* where the condition is given by $\text{Spin } X$. The orange arched arrows denote Workers doing computational work. Finally, the dark green arrows represent the Workers returning to the post-initialization state to repeat for the next CPU cycle during a shot.

from the Manager to the Workers.

2. During Shot Calculation

Entering the CPU cycle during a shot after the blue horizontal block, the Manager has previously notified the Workers that the shot has begun, or all previous work has been completed in the previous cycle. The Manager waits for the workers to respond by waiting for $\text{Ready} > 1$ to become *false*. At this point, each Worker notifies the Manager they are ready by reducing Ready by 1, as indicated by the horizontal green lines directed from Workers to the Manager, and will spin until $\text{Ready} > 0$ is *false*.

Once all of the Workers have communicated readiness to the Manager, the Manager sets Ready to 0 and distributes the work to be calculated, such as the rt-TORBEAM or rt-STRIDE calculation, as seen in the bright green arrow that is directed from the Manager to the Workers. The Manager also sets Complete to the total number of Workers plus 1 and waits for $\text{Complete} > 1$ to be *false*. Now, each Worker receives their work from the Manager, observes $\text{Ready} = 0$ and begins their work. When a Worker completes their work, they communicate back to the Manager to decrement Complete by 1 and each Worker waits for the remaining Workers to

complete their work, which is when $\text{Complete} > 0$ is *false*.

Finally at the end of the cycle, the Manager gathers the results of the calculations and prepares the Workers for the next CPU cycle. When $\text{Complete} > 1$ becomes *false*, all workers have completed their work and the Manager sets Complete to 0 to indicate all Workers have finished and sets Ready to the number of Workers plus 1 to reset the state for the start of the next cycle. At this point, the Manager can do any additional calculations required by the algorithm or communicate results with other PCS algorithms that want the results of the parallelized calculation.

A key point is that the Workers end up in the same state at the end of a CPU cycle as they were after the pre-shot initialization. This guarantees robust thread management and no undefined or unexpected behavior of individual threads.

III. TORBEAM RAY TRACING

Real-time ECH ray tracing is seen as a requirement for accurate ECH aiming to deposit electron cyclotron current drive (ECCD) at rational surfaces for active NTM control^{33–36} as well as a variety of other tasks utilizing ECH and ECCD such as sawtooth control^{37–41}, impurity screening^{42,43}, or ELM control^{44,45}. Combined with a basic feedback controller,

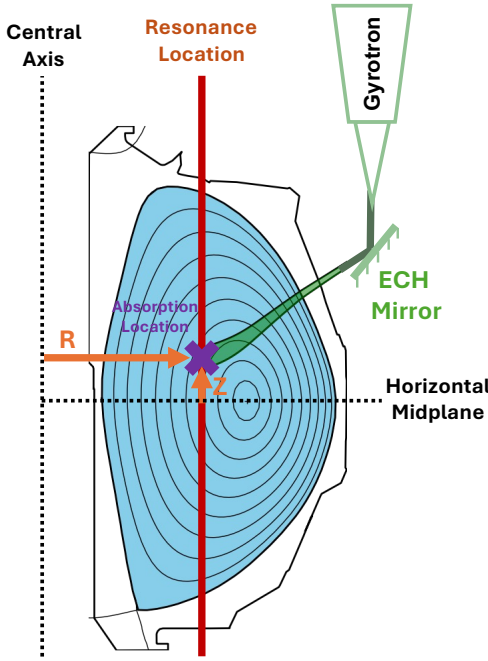


FIG. 2. Example ECH ray-tracing where ECH beam begins from the gyrotron, makes its way to the ECH mirror to be launched into the plasma at some poloidal and toroidal angle. It then travels through the plasma at a calculated trajectory until being absorbed at the vertical red resonance location. The maximum absorption location (purple X), is given by coordinates (R, Z) . Refer to Poli et al.¹⁹ for further explanation.

rt-TORBEAM can be used to accurately steer ECH rays to desired locations in the plasma. This section describes the implementation of the rt-TORBEAM code in section III A followed by experimental deployment in section III B.

A. Problem formulation and real-time implementation

Each gyrotron on DIII-D has an independent, steerable mirror that aims the ECH ray into the plasma. The rt-TORBEAM code calculates its trajectory until the location of maximum absorption is found or the ray leaves the plasma boundary, the last closed flux surface, as visualized in Figure 2. Since each gyrotron launchers and ray trace is fully independent, rt-TORBEAM can be run for all gyrotron launchers in parallel to use the multi-threading library.

Note that a main difference between the offline and rt-TORBEAM code is the simplification from a Gaussian beam to a single ray. This means the full ECH and ECCD deposition profiles are not calculated by rt-TORBEAM, only the (R, Z) location of maximum absorption is calculated to properly steer the ECH mirror. One option to overcome this would be to run rt-TORBEAM multiple times to simulate a Gaussian beam. Another option, and perhaps more straightforward, would be to utilize machine learning surrogate models to calculate the ECH and ECCD profiles directly²⁸.

For our application of ECH mirror steering, the user pro-

vides a spatial coordinate ρ location, ρ_{target} , and the standard rt-TORBEAM library calculates the (R, Z) location of maximum absorption which is converted to a $\rho_{torbeam}$ value based from the real-time equilibria¹⁴. ρ is defined as $\rho = \sqrt{\Phi_N}$ where Φ_N is the normalized toroidal flux to 0 in the core and 1 at the last closed flux surface. The difference in $\rho_{target} - \rho_{torbeam}$ is used to change the mirror angle so that the ρ value calculated from rt-TORBEAM matches the desired ρ_{target} value. This steering algorithm was originally implemented in Kolemen et al.³³.

B. Experimental results

The experimental results from the rt-TORBEAM deployment are shown in Figure 3. In these results, we only show the results from the rt-TORBEAM calculation as the real-time code has been adequately validated in Poli et al.¹⁹. These results show ρ tracking for a single mirror and similar results are seen across all steered gyrotron mirrors. The results show reasonable ρ tracking to within $|\rho_{target} - \rho_{torbeam}| \leq 0.05$.

Figure 3.a shows constant ρ_{target} values for each of the four controlled gyrotrons and the achieved $\rho_{torbeam}$ for each of them. The gyrotron mirrors are slow to move and required approximately 0.5 s to move from their initial position at $\rho = 0.6$ to their respective ρ_{target} values and would require redesigning the mirror steering hardware to further speed up. There is also some minor steady-state error which is attributed to the differences in real-time equilibria used for control and the offline reproduction of the real-time equilibria used for the conversion from (R, Z) to ρ . Finally, it is worth noting that there is more fluctuation in the $\rho = 0.95$ target value close to the plasma edge. Near the plasma edge, the ECH deposition is more effected by density fluctuations and a faster real-time calculation and faster mirror hardware would be required to have improved ρ tracking.

Figure 3.b shows a triangle waveform for ρ_{target} used for all four gyrotrons. While tracking is good during the center when it initially matches ρ_{target} at 3.2 s, it is clear the mirror were too slow to follow the desired ρ_{target} in the two downward slope sections. A gentler slope for ρ_{target} would be needed for improved tracking, or an improved model-based control scheme would be needed to reduce the lag in ρ tracking. Additionally, it is clear at 5 s that the mirror struggles to change directions quickly so sharp changes in ρ_{target} seen here are not desirable for the current controller.

The cycle time plot in Figure 3.c shows continuous computation in around 20 ms for the 4 gyrotron mirror that were steered in this experiment. Due to the parallel nature of adding additional gyrotrons and utilization of the multi-threading library, the 20 ms cycle time will stay constant as DIII-D expands gyrotrons as long as there is a free worker thread for every steered gyrotron mirror. At 5 s there is a large spike in the CPU cycle time where it jumps from the consistent 20 ms up to nearly 40 ms. This large spike is attributed to the rt-TORBEAM code rather than the multi-threading library and further improvements to the rt-TORBEAM code should be able to limit the effect of edge cases greatly increasing exe-

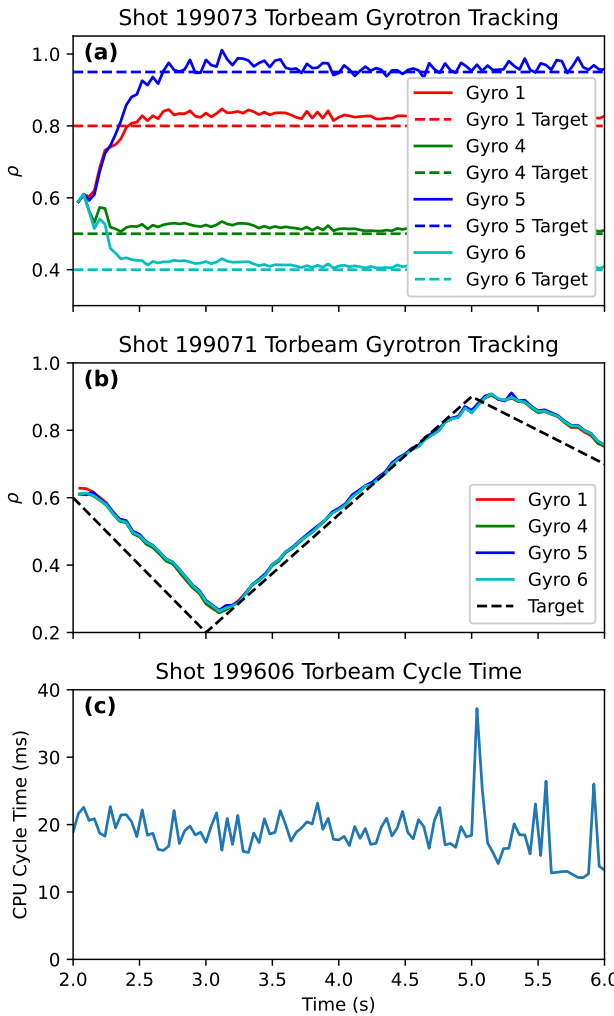


FIG. 3. Experimental results of rt-TORBEAM calculation and gyrotron mirror control. (a) DIII-D shot 199073 with constant ρ_{target} values for four controlled gyrotron mirror where for each individual gyrotron, ρ_{target} (dashed line) and $\rho_{torbeam}$ (solid line) have matching colors. (b) DIII-D shot 199071 with dynamic ρ_{target} (black dashed line) that is the same across all gyrotrons (solid colored lines). (c) CPU cycle time to compute rt-TORBEAM for all four gyrotrons.

cution times.

IV. STRIDE IDEAL STABILITY

The STRIDE code calculates the ideal stability δW parameter and inform real-time controllers if the plasma is in danger of surpassing ideal stability limits. This paper will not analyze the accuracy or validity of the calculation as STRIDE has been benchmarked against similar codes in Glasser et al.²² and Glasser and Kolemen²⁰. Adding additional difficulty in benchmarking the real-time versus offline implementation is the differences in equilibria calculated in real-time versus similar faux “real-time” equilibria calculated post-experiment.

While these differences are minor, it has been shown STRIDE is extremely sensitive to equilibria and we would not expect results to align⁴⁶.

In the following sections, we begin with discussing the changes to the problem formulation that enables rt-STRIDE to be parallelized in real-time in section IV A and then show experimental results of the calculation in section IV B.

A. STRIDE Calculation in real-time

The key insight that enables a real-time calculation with STRIDE is the reformulation of the ideal stability problem as a Riccati equation rather than a Newcomb equation. This enables us to solve for the state transition matrix (STM), denoted by Φ with the useful numerical properties that enable starting at some arbitrary initial conditions

$$\mathbf{u}(0) = \Phi(0)\mathbf{c} \quad (1)$$

$$\mathbf{u}(\psi) = \Phi(\psi)\mathbf{c} = \Phi(\psi)\mathbf{u}(0) \quad (2)$$

the ability to enable us to linearly combine STMs

$$\mathbf{u}(\psi_2) = \Phi(\psi_2)\mathbf{u}(\psi_0) = \Phi(\psi_2, \psi_1)\Phi(\psi_1, \psi_0)\mathbf{u}(\psi_0) \quad (3)$$

and finally the ability to easily switch between forward and backward integration

$$\Phi(\psi_1, \psi_0) = \Phi(\psi_0, \psi_1)^{-1} \quad (4)$$

For a full description of the problem formulation and different numerical methods, look to Glasser et al.²², Glasser et al.²³, and Glasser and Kolemen²⁰.

Because of the above properties of the Riccati problem formulation, STRIDE can solve for the STM by a so-called “shooting” method pictured in Figure 4. Using this shooting method, it was found the STMs are more numerically stable when calculated moving away from rational surfaces⁴⁷. The real-time relevant aspect of the shooting method is the fact that each STM can be calculated independently and combined at the end, based on the properties listed above. This enables us to use the multi-threading library to let each Worker compute an STM, then the Manager can combine all STMs and calculate the final δW result from the combined STMs.

The final problem to address is how to divide the the intervals so when we distribute the calculations to the Workers they take similar times to calculate each interval’s STM. The integrators used to calculated Φ require smaller and more steps close to rational surfaces, so to estimate the required time a measure of Stiffness was assume of the form

$$St = \sum_s \frac{\alpha}{1 + \beta|\psi - \psi_s|} \quad (5)$$

for an interval centered at ψ , all singular surfaces ψ_s , and tunable parameters α and β . This stiffness is used to set the distances between some a_i and a_{i+1} . α and β were selected to as best as possible equally spread the calculation of STMs across Workers.

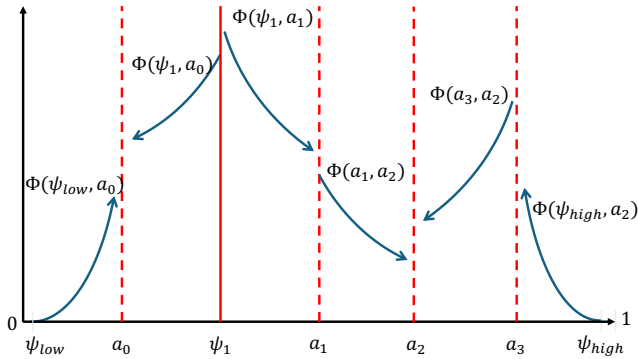


FIG. 4. Shooting method of the STM. Each vertical line represents a cut in the integration of the STM. The solid red lines are rational surfaces where the integration of the STM must be split apart and the dashed red lines being artificial interval breaks to create more intervals to divide the calculation further for the Workers. This figure has been adapted from a similar figure in Glasser and Kolemen²⁰.

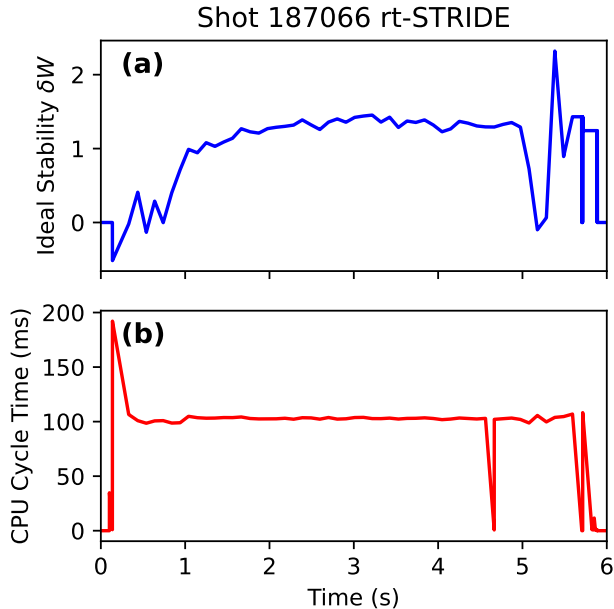


FIG. 5. Results from rt-STRIDE calculation in the DIII-D PCS in shot 187066. (a) gives the δW stability value over time during the shot and (b) shows the CPU cycle time required for one full rt-STRIDE calculation.

B. Experimental results

In experiment, rt-STRIDE ran on a 72 core CPU with approximately 200 intervals where the STM need be computed. With this approach, rt-STRIDE was consistently calculated in approximately 100 ms as seen in Figure 5.b with δW values given in Figure 5.a. There are discrepancies at the beginning and end of the shot and these are attributed to lower quality equilibria causing numerical issues during the plasma current ramp-up and ramp-down.

Additional testing and benchmarking found that the STM integration time was approximately 20 ms of the total 100 ms and the majority of the computation time was spent in the serial data pre-processing calculation of equilibrium coordinates to flux coordinates. The largest possible speed-up would likely be parallelizing this data pre-processing, but further speed-ups could be made with newer hardware with faster processors or more cores.

V. CONCLUSIONS

Two real-time physics codes were efficiently deployed on the DIII-D PCS with a newly implemented, real-time safe multi-threading library. This provided a significant speed-up of these codes to fusion power plant relevant control of ECH power deposition and current drive as well as real-time ideal stability limits. Without the multi-threading capability, these physics codes would not be able to calculate on time-scales relevant for plasma control.

Future real-time physics-based codes can also leverage this multi-threading library to enable faster real-time calculations of vertical stability⁴⁸, other methods for finding ideal wall MHD stability⁴⁹, or physics-based profile prediction and control^{17,50-52}. Emphasis should be placed on developing physic-based codes that can be parallelized and take advantage of CPU multi-threading or GPU processing. Additionally, machine-learning based models that utilize ensemble averaging^{53,54} can utilize the individual threads to run independent models and allow the Manager to aggregate model results.

Development and improvements made to real-time codes are crucial for future fusion power plants. Unlike fast machine learning surrogate models, real-time physics codes have robust performance guarantees on day one of operation and can be relied upon without worry of depending on extrapolation techniques. Due to the extra computational costs of physics-based models, additional effort must be devoted to writing efficient PCS code that is deterministic and reliable for error-free, continuous PCS operation.

ACKNOWLEDGMENTS

This material is based upon work supported by the U.S. Department of Energy, Office of Science, Office of Fusion Energy Sciences, using the DIII-D National Fusion Facility, a DOE Office of Science user facility, under Award DE-FC02-04ER54698. Additionally, this material is supported by the U.S. Department of Energy, under Award DE-SC0015480. Additionally, this material is supported by the National Science Foundation Graduate Research Fellowship under Grant No. DGE-2039656.

We would like to acknowledge the help from E. Poli and M. Reich in their help of the real-time implementation of the TORBEAM code. We would also like to acknowledge the help from A.S. Glasser and A.H. Glasser for their support of the real-time implementation of the STRIDE code.

DISCLAIMER

This report was prepared as an account of work sponsored by an agency of the United States Government. Neither the United States Government nor any agency thereof, nor any of their employees, makes any warranty, express or implied, or assumes any legal liability or responsibility for the accuracy, completeness, or usefulness of any information, apparatus, product, or process disclosed, or represents that its use would not infringe privately owned rights. Reference herein to any specific commercial product, process, or service by trade name, trademark, manufacturer, or otherwise does not necessarily constitute or imply its endorsement, recommendation, or favoring by the United States Government or any agency thereof. The views and opinions of authors expressed herein do not necessarily state or reflect those of the United States Government or any agency thereof.

REFERENCES

¹R.J. Buttery, J.M. Park, J.T. McClenaghan, D. Weisberg, J. Canik, J. Ferron, A. Garofalo, C.T. Holcomb, J. Leuer, and P.B. Snyder. The advanced tokamak path to a compact net electric fusion pilot plant. *Nuclear Fusion*, 61(4):046028, April 2021. ISSN 0029-5515, 1741-4326. doi:10.1088/1741-4326/abe4af. URL <https://iopscience.iop.org/article/10.1088/1741-4326/abe4af>.tex.ids=buttery_advanced_2021-1, buttery_advanced_2021-2.

²A. Hassanein and V. Sizuk. Potential design problems for ITER fusion device. *Scientific Reports*, 11(1):2069, January 2021. ISSN 2045-2322. doi:10.1038/s41598-021-81510-2. URL <https://www.nature.com/articles/s41598-021-81510-2>.

³A. J. Creely, M. J. Greenwald, S. B. Ballinger, D. Brunner, J. Canik, J. Doody, T. Fülop, D. T. Garnier, R. Granetz, T. K. Gray, C. Holland, N. T. Howard, J. W. Hughes, J. H. Irby, V. A. Izzo, G. J. Kramer, A. Q. Kuang, B. LaBombard, Y. Lin, B. Lipschultz, N. C. Logan, J. D. Lore, E. S. Marmar, K. Montes, R. T. Mumgaard, C. Paz-Soldan, C. Rea, M. L. Reinke, P. Rodriguez-Fernandez, K. Särkimäki, F. Sciortino, S. D. Scott, A. Snicker, P. B. Snyder, B. N. Sorbom, R. Sweeney, R. A. Tinguely, E. A. Tolman, M. Umansky, O. Vallhagen, J. Varje, D. G. Whyte, J. C. Wright, S. J. Wukitch, J. Zhu, and the SPARC Team. Overview of the SPARC tokamak. *Journal of Plasma Physics*, 86(5):865860502, October 2020. ISSN 0022-3778, 1469-7807. doi:10.1017/S0022377820001257. URL https://www.cambridge.org/core/product/identifier/S0022377820001257/type/journal_article.

⁴M. Lennholm, T. Budd, R. Felton, M. Gadeberg, A. Goodyear, F. Milani, and F. Sartori. Plasma control at JET. *Fusion Engineering and Design*, 48(1-2):37–45, August 2000. ISSN 09203796. doi:10.1016/S0920-3796(00)00125-3. URL <https://linkinghub.elsevier.com/retrieve/pii/S0920379600001253>.

⁵O. Kudlacek, P. David, I. Gomez, A. Gräter, B. Sieglin, W. Treutterer, M. Weiland, T. Zehetbauer, M. Van Berkel, M. Bernert, T. Bosman, F. Felici, L. Giannone, J. Illerhaus, D. Kropackova, P.T. Lang, M. Maraschek, B. Ploeckl, M. Reich, A. Vedl Kubincova, the ASDEX Upgrade Team, and EUROfusion Tokamak Exploitation Team. Overview of advances in ASDEX Upgrade plasma control to support critical physics research for ITER and beyond. *Nuclear Fusion*, 64(5):056012, May 2024. ISSN 0029-5515, 1741-4326. doi:10.1088/1741-4326/ad3472. URL <https://iopscience.iop.org/article/10.1088/1741-4326/ad3472>.

⁶L.L. Yan, Q.P. Yuan, B.J. Xiao, R.R. Zhang, Y.Y. Zheng, J.Q. Zhu, and H.R. Guo. Custom application of PCS software development platform on EAST. *Fusion Engineering and Design*, 166:112314, May 2021. ISSN 09203796. doi:10.1016/j.fusengdes.2021.112314. URL <https://linkinghub.elsevier.com/retrieve/pii/S0920379621000909>.

⁷I. Yonekawa, Y. Kawamata, T. Totsuka, H. Akasaka, M. Sueoka, and H. Yoshida. Current status and future prospects of the JT-60U control system. *Fusion Engineering and Design*, 71(1-4):11–15, June 2004. ISSN 09203796. doi:10.1016/j.fusengdes.2004.04.003. URL <https://linkinghub.elsevier.com/retrieve/pii/S0920379604000158>.

⁸M. Margo, B. Penaflor, H. Shen, J. Ferron, D. Piglowski, P. Nguyen, J. Rauch, M. Clement, A. Battey, and C. Rea. Current State of DIII-D Plasma Control System. *Fusion Engineering and Design*, 150:111368, January 2020. ISSN 09203796. doi:10.1016/j.fusengdes.2019.111368. URL <https://linkinghub.elsevier.com/retrieve/pii/S0920379619308646>.

⁹Cristian Galperti, Federico Felici, Trang Vu, Olivier Sauter, F. Carpanese, M. Kong, G. Marceca, A. Merle, A. Pau, A. Perek, F. Pesamosca, M. Baquero-Ruiz, S. Coda, J. Decker, B. Duval, M. Gospodarczyk, A. Karpushov, S. Marchioni, A. Maier, B. Marletaz, A. Segovia, B. Vincent, C. Yildiz, D. Carnevale, N. Ferron, J. Koenders, B. Kool, G. Manduchi, M. Maraschek, P. Milne, A.C. Neto, E. Poli, T. Ravensbergen, M. Reich, N. Rispoli, and F. Sartori. Overview of the TCV digital real-time plasma control system and its applications. *Fusion Engineering and Design*, 208:114640, November 2024. ISSN 09203796. doi:10.1016/j.fusengdes.2024.114640. URL <https://linkinghub.elsevier.com/retrieve/pii/S0920379624004915>.

¹⁰P.C. De Vries, M. Cinque, G. De Tommasi, W. Treutterer, D. Humphreys, M. Walker, F. Felici, I. Gomez, L. Zabeo, T. Ravensbergen, L. Pangione, F. Rimini, S. Rosiello, Y. Gribov, M. Dubrov, A. Vu, I. Carvalho, W.R. Lee, T. Tak, A. Zagar, R. Gunion, R. Pitts, M. Mattei, A. Pironti, M. Arriola, F. Pesamosca, O. Kudlacek, G. Raupp, G. Pautasso, R. Nouailletas, Ph. Moreau, and D. Weldon. Strategy to systematically design and deploy the ITER plasma control system: A system engineering and model-based design approach. *Fusion Engineering and Design*, 204:114464, July 2024. ISSN 09203796. doi:10.1016/j.fusengdes.2024.114464. URL <https://linkinghub.elsevier.com/retrieve/pii/S092037962400317X>.

¹¹Piotr Perek, Taehyun Tak, Woong-Ryol Lee, Anze Zagar, Dariusz Makowski, Domen Soklic, and Peter Karlovsek. Preliminary design of ITER PCS Provisioning System. *Fusion Engineering and Design*, 220:115348, November 2025. ISSN 09203796. doi:10.1016/j.fusengdes.2025.115348. URL <https://linkinghub.elsevier.com/retrieve/pii/S0920379625005447>.

¹²A. J. Creely, D. Brunner, R. T. Mumgaard, M. L. Reinke, M. Segal, B. N. Sorbom, and M. J. Greenwald. SPARC as a platform to advance tokamak science. *Physics of Plasmas*, 30(9):090601, September 2023. ISSN 1070-664X, 1089-7674. doi:10.1063/5.0162457. URL <https://pubs.aip.org/pop/article/30/9/090601/2909870/SPARC-as-a-platform-to-advance-tokamak-science>.

¹³Sang-hee Hahn, H. Han, M.H. Woo, J.G. Bak, J. Chung, Y.M. Jeon, J.H. Jeong, M. Joung, J.W. Juhn, H.S. Kim, Heungsu Kim, M.W. Lee, G.W. Shin, T.H. Tak, S.W. Yoon, J. Barr, N.W. Eidiets, D.A. Humphreys, A. Hyatt, B.G. Penaflor, D.A. Piglowski, M.L. Walker, A.S. Welander, M.D. Boyer, K. Erickson, and D. Mueller. Advances and challenges in KSTAR plasma control toward long-pulse, high-performance experiments. *Fusion Engineering and Design*, 156:111622, July 2020. ISSN 09203796. doi:10.1016/j.fusengdes.2020.111622. URL <https://linkinghub.elsevier.com/retrieve/pii/S0920379620301708>.

¹⁴J.R. Ferron, M.L. Walker, L.L. Lao, H.E. St John, D.A. Humphreys, and J.A. Leuer. Real time equilibrium reconstruction for tokamak discharge control. *Nuclear Fusion*, 38(7):1055–1066, July 1998. ISSN 0029-5515. doi:10.1088/0029-5515/38/7/308. URL <https://iopscience.iop.org/article/10.1088/0029-5515/38/7/308>.

¹⁵J.-M. Moret, B.P. Duval, H.B. Le, S. Coda, F. Felici, and H. Reimerdes. Tokamak equilibrium reconstruction code LIUQE and its real time implementation. *Fusion Engineering and Design*, 91:1–15, February 2015. ISSN 09203796. doi:10.1016/j.fusengdes.2014.09.019. URL <https://linkinghub.elsevier.com/retrieve/pii/S0920379614005973>.

¹⁶C. Piron, F. Felici, B. Faugeras, N. Ferron, G. Manduchi, N. Marconato, C. Meekes, L. Piron, Z. Stancar, D. Valcarcel, D. Voltolina, and M. Weiland. Development of the RAPTOR suite of codes towards real-time reconstruction of JET discharges. *Fusion Engineering and Design*, 169:112431, August 2021. ISSN 09203796. doi:10.1016/j.fusengdes.2021.112431. URL <https://linkinghub.elsevier.com/retrieve/pii/S0920379621002076>.

¹⁷F. Felici, O. Sauter, S. Coda, B.P. Duval, T.P. Goodman, J-M. Moret, and J.I. Paley. Real-time physics-model-based simulation of the current density profile in tokamak plasmas. *Nuclear Fusion*, 51(8): 083052, August 2011. ISSN 0029-5515, 1741-4326. doi:10.1088/0029-5515/51/8/083052. URL <https://iopscience.iop.org/article/10.1088/0029-5515/51/8/083052>.

¹⁸M. Weiland, R. Bilato, R. Dux, B. Geiger, A. Lebschy, F. Felici, R. Fischer, D. Rittich, M. van Zeeland, the ASDEX Upgrade Team, and the Eurofusion MST1 Team. RABBIT: Real-time simulation of the NBI fast-ion distribution. *Nuclear Fusion*, 58(8): 082032, August 2018. ISSN 0029-5515, 1741-4326. doi:10.1088/1741-4326/aaabf0f. URL <https://iopscience.iop.org/article/10.1088/1741-4326/aaabf0f>. tex.ids: weiland_rabbit_2018.

¹⁹E. Poli, A. Bock, M. Lochbrunner, O. Maj, M. Reich, A. Snicker, A. Stegmeir, F. Volpe, N. Bertelli, R. Bilato, G.D. Conway, D. Farina, F. Felici, L. Figini, R. Fischer, C. Galperti, T. Happel, Y.R. Lin-Liu, N.B. Marushchenko, U. Mszanowski, F.M. Poli, J. Stober, E. Westerhof, R. Zille, A.G. Peeters, and G.V. Pereverzev. TORBEAM 2.0, a paraxial beam tracing code for electron-cyclotron beams in fusion plasmas for extended physics applications. *Computer Physics Communications*, 225:36–46, April 2018. ISSN 00104655. doi:10.1016/j.cpc.2017.12.018. URL <https://linkinghub.elsevier.com/retrieve/pii/S001046551730423X>.

²⁰Alexander S. Glasser and Egemen Kolemen. A robust solution for the resistive MHD toroidal δ' matrix in near real-time. *Physics of Plasmas*, 25(8):082502, August 2018. ISSN 1070-664X, 1089-7674. doi:10.1063/1.5029477. URL <https://pubs.aip.org/pop/article/25/8/082502/1058163/A-robust-solution-for-the-resistive-MHD-toroidal>.

²¹A H Glasser. The direct criterion of Newcomb for the ideal MHD stability of an axisymmetric toroidal plasma. *Phys. Plasmas*, 23(7): 72505, 2016. ISSN 1070-664X, 1089-7674. doi:10.1063/1.4958328. URL <https://pubs.aip.org/pop/article/23/7/072505/594703/The-direct-criterion-of-Newcomb-for-the-ideal-MHD>.

²²Alexander S. Glasser, Egemen Kolemen, and A. H. Glasser. A Riccati solution for the ideal MHD plasma response with applications to real-time stability control. *Physics of Plasmas*, 25(3):032507, March 2018. ISSN 1070-664X, 1089-7674. doi:10.1063/1.5007042. URL <https://pubs.aip.org/pop/article/25/3/032507/1060307/A-Riccati-solution-for-the-ideal-MHD-plasma>.

²³Alexander S. Glasser, A. H. Glasser, Rory Conlin, and Egemen Kolemen. An ideal MHD δw stability analysis that bypasses the Newcomb equation. *Physics of Plasmas*, 27(2):022114, February 2020. ISSN 1070-664X, 1089-7674. doi:10.1063/1.5109160. URL <http://aip.scitation.org/doi/10.1063/1.5109160>. tex.ids= glasser_ideal_2020-1.

²⁴OpenMP Architecture Review Board. OpenMP application program interface version 3.0, May 2008. URL <http://www.openmp.org/mp-documents/spec30.pdf>.

²⁵Rory Conlin, Keith Erickson, Joseph Abbate, and Egemen Kolemen. Keras2c: A library for converting Keras neural networks to real-time compatible C. *Engineering Applications of Artificial Intelligence*, 100:104182, April 2021. ISSN 09521976. doi:10.1016/j.engappai.2021.104182. URL <https://linkinghub.elsevier.com/retrieve/pii/S0952197621000294>.

²⁶Andrew Rothstein, Hiro Joseph Farre-Kaga, Jalal Butt, Ricardo Shousha, Keith Erickson, Takuma Wakatsuki, Azaraksh Jalalvand, Peter Steiner, Sangkyeon Kim, and Egemen Kolemen. Enabling integrated ai control on diii-d. Under submission, 2025.

²⁷Mark D Boyer, Cristina Rea, and Mitchell D Clement. Toward active disruption avoidance via real-time estimation of the safe operating region and disruption proximity in tokamaks. *Nuclear Fusion*, November 2021. ISSN 0029-5515, 1741-4326. doi:10.1088/1741-4326/ac359e. URL <https://iopscience.iop.org/article/10.1088/1741-4326/ac359e>. tex.ids= boyer_toward_2021.

²⁸Andrew Rothstein, Minseok Kim, Minho Woo, Minsoo Cha, Cheolsik Byun, Sangkyeon Kim, Keith Erickson, Youngho Lee, Josh Josephy-Zack, Jalal Butt, Ricardo Shousha, Mi Joung, June-Woo Juhn, Kyu-Dong Lee, and Egemen Kolemen. TorbeamNN: machine learning-based steering of ECH mirrors on KSTAR. *Plasma Physics and Controlled Fusion*, 67(5):055036, May 2025. ISSN 0741-3335, 1361-6587. doi:10.1088/1361-6587/add08b. URL <https://iopscience.iop.org/> article/10.1088/1361-6587/add08b.

²⁹Jaemin Seo, SangKyeun Kim, Azaraksh Jalalvand, Rory Conlin, Andrew Rothstein, Joseph Abbate, Keith Erickson, Josiah Wai, Ricardo Shousha, and Egemen Kolemen. Avoiding fusion plasma tearing instability with deep reinforcement learning. *Nature*, 626(8000):746–751, February 2024. ISSN 0028-0836, 1476-4687. doi:10.1038/s41586-024-07024-9. URL <https://www.nature.com/articles/s41586-024-07024-9>.

³⁰Rushil Anirudh, Rick Archibald, M. Salman Asif, Markus M. Becker, Sadruddin Benkadda, Peer-Timo Bremer, Rick H. S. Budé, C. S. Chang, Lei Chen, R. M. Churchill, Jonathan Citrin, Jim A. Gaffney, Ana Gainaru, Walter Gekelman, Tom Gibbs, Satoshi Hamaguchi, Christian Hill, Kelli Humbird, Sören Jalas, Satoru Kawaguchi, Gon-Ho Kim, Manuel Kirchen, Scott Klasky, John L. Kline, Karl Krushelnick, Bogdan Kustowski, Giovanni Lapenta, Wenting Li, Tammy Ma, Nigel J. Mason, Ali Mesbah, Craig Michoski, Todd Munson, Izumi Murakami, Habib N. Najm, K. Erik J. Olofsson, Seolhye Park, J. Luc Peterson, Michael Probst, David Pugmire, Brian Sammuli, Kapil Sawlani, Alexander Scheinker, David P. Schissel, Rob J. Shalloo, Jun Shinagawa, Jaegu Seong, Brian K. Spears, Jonathan Tennyson, Jayaraman Thiagarajan, Catalin M. Ticoş, Jan Trieschmann, Jan Van Dijk, Brian Van Essen, Peter Ventzek, Haimin Wang, Jason T. L. Wang, Zhehui Wang, Kristian Wende, Xueqiao Xu, Hiroshi Yamada, Tatsuya Yokoyama, and Xinhua Zhang. 2022 Review of Data-Driven Plasma Science. *IEEE Transactions on Plasma Science*, 51(7):1750–1838, July 2023. ISSN 0093-3813, 1939-9375. doi:10.1109/TPS.2023.3268170. URL <https://ieeexplore.ieee.org/document/10214236/>.

³¹R. M. Churchill, B. Tobias, Y. Zhu, and DIII-D team. Deep convolutional neural networks for multi-scale time-series classification and application to tokamak disruption prediction using raw, high temporal resolution diagnostic data. *Physics of Plasmas*, 27(6):062510, June 2020. ISSN 1070-664X, 1089-7674. doi:10.1063/1.5144458. URL <http://aip.scitation.org/doi/10.1063/1.5144458>.

³²Keith G. Erickson, Gregory J. Tchilinguirian, Ronald E. Hatcher, and William M. Davis. NSTX-U Digital Coil Protection System Software Detailed Design. *IEEE Transactions on Plasma Science*, 42(6):1811–1818, June 2014. ISSN 0093-3813, 1939-9375. doi:10.1109/TPS.2014.2321106. URL <http://ieeexplore.ieee.org/document/6822612/>.

³³E. Kolemen, R. Ellis, R.J. La Haye, D.A. Humphreys, J. Lohr, S. Noraky, B.G. Penafior, and A.S. Welander. Real-time mirror steering for improved closed loop neoclassical tearing mode suppression by electron cyclotron current drive in DIII-D. *Fusion Engineering and Design*, 88(11):2757–2760, November 2013. ISSN 09203796. doi:10.1016/j.fusengdes.2013.02.168. URL <https://linkinghub.elsevier.com/retrieve/pii/S0920379613002834>.

³⁴H Zohm, G Ganterbein, F Leuterer, A Manini, M Maraschek, Q Yu, and The Asdex Upgrade Team. Control of MHD instabilities by ECCD: ASDEX Upgrade results and implications for ITER. *Nuclear Fusion*, 47(3): 228–232, March 2007. ISSN 0029-5515, 1741-4326. doi:10.1088/0029-5515/47/3/010. URL <https://iopscience.iop.org/article/10.1088/0029-5515/47/3/010>.

³⁵O Sauter, M A Henderson, G Ramponi, H Zohm, and C Zucca. On the requirements to control neoclassical tearing modes in burning plasmas. *Plasma Physics and Controlled Fusion*, 52(2):025002, February 2010. ISSN 0741-3335, 1361-6587. doi:10.1088/0741-3335/52/2/025002. URL <https://iopscience.iop.org/article/10.1088/0741-3335/52/2/025002>.

³⁶Y S Park, M H Woo, S A Sabbagh, H S Han, B H Park, J S Kang, and H S Kim. Initial results from neoclassical tearing mode stabilization experiment in KSTAR high normalized beta plasmas. *Plasma Physics and Controlled Fusion*, 66(12):125013, December 2024. ISSN 0741-3335, 1361-6587. doi:10.1088/1361-6587/ad8a8a. URL <https://iopscience.iop.org/article/10.1088/1361-6587/ad8a8a>.

³⁷F. Felici, T.P. Goodman, O. Sauter, G. Canal, S. Coda, B.P. Duval, and J.X. Rossel. Integrated real-time control of MHD instabilities using multi-beam ECRH/ECCD systems on TCV. *Nuclear Fusion*, 52(7): 074001, July 2012. ISSN 0029-5515, 1741-4326. doi:10.1088/0029-5515/52/7/074001. URL <https://iopscience.iop.org/article/10.1088/0029-5515/52/7/074001>.

³⁸T. P. Goodman, F. Felici, O. Sauter, and J. P. Graves. Sawtooth Pacing by Real-Time Auxiliary Power Control in a Tokamak Plasma. *Physical Review Letters*, 106(24):245002, June 2011. ISSN 0031-9007, 1079-7114. doi:

10.1103/PhysRevLett.106.245002. URL <https://link.aps.org/doi/10.1103/PhysRevLett.106.245002>.

³⁹M. Maraschek, G. Gantenbein, T.P. Goodman, S. Günter, D.F. Howell, F. Leuterer, A. Mück, O. Sauter, H. Zohm, Contributors To The Efda-Jet Workprogramme, and The Asdex Upgrade Team. Active control of MHD instabilities by ECCD in ASDEX Upgrade. *Nuclear Fusion*, 45(11):1369–1376, November 2005. ISSN 0029-5515, 1741-4326. doi:10.1088/0029-5515/45/11/018. URL <https://iopscience.iop.org/article/10.1088/0029-5515/45/11/018>.

⁴⁰M. Lennholm, L.-G. Eriksson, F. Turco, F. Bouquey, C. Darbos, R. Dumont, G. Giruzzi, M. Jung, R. Lambert, R. Magne, D. Molina, P. Moreau, F. Rimini, J.-L. Segui, S. Song, and E. Traisnel. Closed Loop Sawtooth Period Control Using Variable ECCD Injection Angles on Tore Supra. *Fusion Science and Technology*, 55(1):45–55, January 2009. ISSN 1536-1055, 1943-7641. doi:10.13182/FST09-A4052. URL <https://www.tandfonline.com/doi/full/10.13182/FST09-A4052>.

⁴¹M. Lennholm, D. Frigione, J.P. Graves, P.S. Beaumont, T. Blackman, I.S. Carvalho, I. Chapman, R. Dumont, R. Felton, L. Garzotti, M. Goniche, A. Goodyear, D. Grist, S. Jachmich, T. Johnson, P. Lang, E. Lerche, E. De La Luna, I. Monakhov, R. Mooney, J. Morris, M.F.F. Nave, M. Reich, F. Rimini, G. Sips, H. Sheikh, C. Sozzi, M. Tsallas, and JET Contributors. Real-time control of ELM and sawtooth frequencies: similarities and differences. *Nuclear Fusion*, 56(1):016008, January 2016. ISSN 0029-5515, 1741-4326. doi:10.1088/0029-5515/56/1/016008. URL <https://iopscience.iop.org/article/10.1088/0029-5515/56/1/016008>.

⁴²R. Dux, R. Neu, A.G. Peeters, G. Pereverzev, A.M. Ck, F. Ryter, J. Stober, and Asdex Upgrade Team. Influence of the heating profile on impurity transport in ASDEX Upgrade. *Plasma Physics and Controlled Fusion*, 45(9):1815–1825, September 2003. ISSN 0741-3335, 1361-6587. doi:10.1088/0741-3335/45/9/317. URL <https://iopscience.iop.org/article/10.1088/0741-3335/45/9/317>.

⁴³T. Odstrčil, N.T. Howard, F. Sciortino, C. Chrystal, C. Holland, E. Hollmann, G. McKee, K.E. Thome, and T.M. Wilks. Dependence of the impurity transport on the dominant turbulent regime in ELM-y H-mode discharges on the DIII-D tokamak. *Physics of Plasmas*, 27(8):082503, August 2020. ISSN 1070-664X, 1089-7674. doi:10.1063/5.0010725. URL <https://pubs.aip.org/pop/article/27/8/082503/1023860/Dependence-of-the-impurity-transport-on-the>.

⁴⁴N.C. Logan, B.C. Lyons, M. Knolker, Q. Hu, T. Cote, and P. Snyder. Access to stable, high pressure tokamak pedestals using local electron cyclotron current drive. *Nuclear Fusion*, 64(1):014003, January 2024. ISSN 0029-5515, 1741-4326. doi:10.1088/1741-4326/ad0fbe. URL <https://iopscience.iop.org/article/10.1088/1741-4326/ad0fbe>.

⁴⁵Q.M. Hu, N.C. Logan, Q. Yu, and A. Bortolon. Effects of edge-localized electron cyclotron current drive on edge-localized mode suppression by resonant magnetic perturbations in DIII-D. *Nuclear Fusion*, 64(4):046027, April 2024. ISSN 0029-5515, 1741-4326. doi:10.1088/1741-4326/ad2ca8. URL <https://iopscience.iop.org/article/10.1088/1741-4326/ad2ca8>.

⁴⁶Andrew Rothstein, Vikram Alliani, Kate Krogen, Xuan Sun, Minseok Kim, William Boyes, Nik Logan, Anthony Xing, Egemen Kolemen, and the DIII-D Team. Assessing the numerical stability of physics models to equilibrium variation through database comparisons. *Plasma Physics and Controlled Fusion*, to appear:055036, May 2025. doi:to appear.

⁴⁷Rory Conlin, Keith Erickson, Jayson Barr, Joseph Abbate, Alex Glasser, and Egemen Kolemen. Real time mhd stability analysis and control with stride. In *MHD Workshop Proceedings*. Presented as the 3DSP Meeting at General Atomics, 2021.

⁴⁸B.S. Sammuli, J.L. Barr, and D.A. Humphreys. Avoidance of vertical displacement events in DIII-D using a neural network growth rate estimator. *Fusion Engineering and Design*, 169:112492, August 2021. ISSN 09203796. doi:10.1016/j.fusengdes.2021.112492. URL <https://linkinghub.elsevier.com/retrieve/pii/S0920379621002684>.

⁴⁹SeongMoo Yang, Stefano Munaretto, Tong Liu, Qiming Hu, Christopher Thomas Holcomb, Nikolas C. Logan, Brian S. Victor, Keith Erickson, and Alessandro Bortolon. Stability Evaluation and Mitigation Strategies in Advanced Tokamaks using 3D MHD Spectroscopy. *Nuclear Fusion*, August 2025. ISSN 0029-5515, 1741-4326. doi:10.1088/1741-4326/adf6c9. URL <https://iopscience.iop.org/article/10.1088/1741-4326/adf6c9>.

⁵⁰F. Carpanese, F. Felici, C. Galperti, A. Merle, J.M. Moret, O. Sauter, and TCV. First demonstration of real-time kinetic equilibrium reconstruction on TCV by coupling LIUQE and RAPTOR. *Nuclear Fusion*, 60(6):066020, June 2020. ISSN 0029-5515, 1741-4326. doi:10.1088/1741-4326/ab81ac. URL <https://iopscience.iop.org/article/10.1088/1741-4326/ab81ac>.

⁵¹Shira Morosohk, Andres Pajares, and Eugenio Schuster. Estimation of the Electron Temperature Profile in Tokamaks Using Analytical and Neural Network Models. In *2022 American Control Conference (ACC)*, pages 278–283, Atlanta, GA, USA, June 2022. IEEE. ISBN 978-1-6654-5196-3. doi:10.23919/ACC53348.2022.9867844. URL <https://ieeexplore.ieee.org/document/9867844>.

⁵²S. Morosohk, Z. Wang, S.T. Paruchuri, T. Rafiq, and E. Schuster. Simultaneous control of the electron temperature and safety factor profiles in DIII-D using model-based optimal control techniques. *Plasma Physics and Controlled Fusion*, 67(1):015012, January 2025. ISSN 0741-3335, 1361-6587. doi:10.1088/1361-6587/ad994d. URL <https://iopscience.iop.org/article/10.1088/1361-6587/ad994d>.

⁵³Ricardo Shousha, Jaemin Seo, Keith Erickson, Zichuan Xing, SangKyeun Kim, Joseph Abbate, and Egemen Kolemen. Machine learning-based real-time kinetic profile reconstruction in DIII-D. *Nuclear Fusion*, 64(2):026006, 2023. ISSN 0029-5515, 1741-4326. doi:10.1088/1741-4326/ad142f. URL <https://iopscience.iop.org/article/10.1088/1741-4326/ad142f>. Publisher: IOP Publishing.

⁵⁴Jaemin Seo, Rory Conlin, Andrew Rothstein, SangKyeun Kim, Joseph Abbate, Azarakhs Jalalvand, and Egemen Kolemen. Multimodal Prediction of Tearing Instabilities in a Tokamak. In *2023 International Joint Conference on Neural Networks (IJCNN)*, pages 1–8, Gold Coast, Australia, June 2023. IEEE. ISBN 978-1-6654-8867-9. doi:10.1109/IJCNN54540.2023.10191359. URL <https://ieeexplore.ieee.org/document/10191359>.